Estimation of Surface Energy Balance from Radiant Surface Temperature and NOAA AVHRR Sensor Reflectances over Agricultural and Native Vegetation

HUANG XINMEI AND T. J. LYONS

Environmental Science, Murdoch University, Murdoch, Australia

R. C. G. SMITH

CSIRO, Division of Exploration Geoscience, Wembley, Australia, and Remote Sensing Application Centre, Western Australian Department of Land Administration, Perth, Australia

J. M. HACKER AND P. SCHWERDTFEGER

Flinders Institute for Atmospheric and Marine Sciences, Flinders University of South Australia, Adelaide, Australia

(Manuscript received 24 August 1992, in final form 18 December 1992)

ABSTRACT

A model is developed to evaluate surface heat flux densities using the radiant surface temperature and red and near-infrared reflectances from the NOAA Advanced Very High Resolution Radiometer sensor. Net radiation is calculated from an empirical formulation and albedo estimated from satellite observations. Infrared surface temperature is corrected to aerodynamic surface temperature in estimating the sensible heat flux and the latent flux is evaluated as the residual of the surface energy balance. When applied to relatively homogeneous agricultural and native vegetation, the model yields realistic estimates of sensible and latent heat flux density in the surface layer for cases where either the sensible or latent flux dominates.

1. Introduction

Remote-sensing techniques have been used to estimate the surface energy balance over reasonably large areas in recent years. The combination of both ground-based and remotely sensed observations enables the direct evaluation of net radiation, sensible heat flux, and soil heat flux. Latent heat flux can then be estimated as the residual of the surface energy balance.

The thermal infrared temperature is commonly used to calculate the sensible heat flux. However, if the same value is used for the roughness lengths for heat and momentum, this results in an overestimate of the sensible heat flux in unstable conditions. Alternatively, the aerodynamic temperature can be used in place of the surface temperature, but this leads to systematic errors in the sensible heat flux if the differences between surface aerodynamic temperature and infrared surface temperature (Choudhury et al. 1986; Smith et al. 1989) are not accounted for. During FIFE, Hall et al. (1991) noted that the infrared surface temperature overestimated the aerodynamic surface temperature by approximately 2°C. It is also difficult to evaluate the soil heat flux over large areas from point observations as both soil and land surface conditions vary widely. Fuchs and Hadas (1972) and Novak and Black (1983), among others, suggested a relationship between soil heat flux and net radiation whereas Clothier et al. (1986) and Daughtry et al. (1990) found that the soil heat flux is also a function of the fractional green vegetation cover measured by the normalized difference vegetation index (NDVI).

In the present study, a model is developed to evaluate the surface heat fluxes using the radiant surface temperature and red and near-infrared reflectances from the NOAA Advanced Very High Resolution Radiometer (AVHRR) sensor in relatively homogeneous areas. Net radiation is calculated from an empirical formulation and albedo estimated from satellite observations. Infrared surface temperature is corrected to aerodynamic surface temperature for estimating the sensible heat flux. The predicted sensible and latent heat fluxes are compared to direct in situ observations.

2. Energy balance model

For a vegetated surface, a complete energy balance can be written as (Brutsaert 1982)

$$R_n - \mathrm{LE} - H - G - L_p F_p + A_h = \frac{\partial Q}{\partial t}, \quad (1)$$

Corresponding author address: Dr. T. J. Lyons, Environmental Science, Murdoch University, Murdoch, WA, Australia, 6150.

where R_n is the net radiation, H the sensible heat flux density, LE the latent heat flux density, G the soil heat flux density, L_p the thermal conversion factor for the fixation of CO_2, F_p the specific flux of CO_2, A_h the horizontal energy advection, and Q the energy storage with time t. As energy absorption by photosynthesis, L_pF_p, is usually smaller than 1% of the global radiation, it is within our experimental uncertainty and can be neglected. The rate of energy storage is important at sunrise and sunset when the net radiation is very small, but it can be neglected during the middle of the day. Since the satellite overpass occurs in the early afternoon, in the absence of advection, the surface energy balance is mainly controlled by net radiation, soil, and latent heat fluxes.

Thus, the surface energy balance equation can be written as

$$R_n = G + H + \mathrm{LE}, \tag{2}$$

where R_n, H, and G are calculated from empirical formulations using satellite and surface-based observations, and LE is estimated as the residual. That is, we solve for

$$\mathrm{LE} = R_n - H - G, \tag{3}$$

wherein any residual errors in the determination of R_n, H, and G will be incorporated in the estimate of LE.

Assuming clear sky conditions, net radiation can be expressed as

$$R_n = S_d(1 - A) + F_d - \epsilon\sigma T_s^4, \tag{4}$$

where A is the surface albedo estimated from NOAA AVHRR channel 1 and 2 reflectances following Brest and Goward (1987) and Chen and Ohring (1984); S_d, the incoming solar radiation at the surface, is accounted for as the product of Rayleigh scattering from air molecules, gas absorption, aerosol absorption, and scattering, and is described according to the parameterization of Savijarvi (1990):

$$S_d = S_0\cos(\alpha) \times\left\{1 - 0.024[\cos(\alpha)]^{-0.5} - a_a 0.11\left[\frac{u_z}{\cos(\alpha)}\right]^{0.25} - a_s\left[\frac{0.28}{1 + 6.43\cos(\alpha)} - 0.07A\right]\right\}, \tag{5}$$

where a_s, a_a are the coefficients for aerosol absorption and scattering, respectively, u_z the water vapor pathlength, S_0 the solar constant, and α the solar zenith angle.

The incoming longwave radiation F_d is expressed as (Satterlund 1979)

$$F_d = 1.08\sigma T_a^4[1 - \exp(-e_0^{T_a/2016})], \tag{6}$$

where e_0 is the water vapor pressure (hPa), T_a the air temperature, σ the Stefan–Boltzmann constant, and T_s the infrared surface temperature, which is estimated from satellite observations as (Price 1984)

$$T_s = T_4 + \frac{3.3(T_4 - T_5)(3.5 + \epsilon)}{4.5}, \tag{7}$$

where T_4 and T_5 are the brightness temperatures of NOAA AVHRR channels 4 and 5, respectively, and ϵ is the emissivity of the surface, which we have arbitrarily assumed to be 0.96.

Using similarity theory in the surface layer, the calculation of sensible heat flux requires the potential temperature at the surface roughness level, defined as the aerodynamic potential temperature, rather than the surface potential temperature (Businger 1973). Thus,

$$H = \rho C_p C_h[\theta(z_0) - \theta(z)], \tag{8}$$

where ρ is the air density, C_p the specific heat of air, C_h the heat exchange coefficient, $\theta(z)$ the potential temperature at height z, and $\theta(z_0)$ the aerodynamic potential temperature. Following Zilitinkevich (1970), the expression for $\theta(z_0)$ is

$$\theta(z_0) = \theta_s + 0.0962\frac{\theta_*}{k}\left(\frac{u_* z_0}{\nu}\right)^{0.45}, \tag{9}$$

where ν is the dynamic viscosity coefficient of air, k the von Kármán constant (taken as 0.4), and θ_s the surface potential temperature calculated directly from T_s.

In the surface layer, H can be written as

$$H = -\rho C_p \theta_* u_*. \tag{10}$$

Thus, rearranging the above equations the sensible heat flux can be expressed as

$$H = \frac{\rho C_p C_h[\theta_s - \theta(z)]}{1 + 35.63 C_h z_0^{0.45}/u_*^{0.55}}, \tag{11}$$

where u_*, the friction velocity, is estimated from

$$u_*^2 = C_m u, \tag{12}$$

C_m is the momentum exchange coefficient, and u the mean wind speed.

The exchange coefficients are defined as

$$C_h = k^2 u \mathrm{GH}(z, z_{0m}, z_{0h}, \mathrm{Ri}_B)\left[\ln\left(\frac{z}{z_{0m}}\right)\ln\left(\frac{z}{z_{0h}}\right)\right]^{-1} \tag{13}$$

$$C_m = k^2 u \mathrm{FH}(z, z_{0m}, \mathrm{Ri}_B)\left[\ln\left(\frac{z}{z_{0m}}\right)\ln\left(\frac{z}{z_{0m}}\right)\right]^{-1}, \tag{14}$$

where z_{0m}, z_{0h} are the surface roughnesses for momentum and heat, respectively. Although the overwhelming experimental evidence suggests that $z_{0h} < z_{0m}$ (Brutsaert 1982), Thom and Oliver (1977) pointed out that under many circumstances, the error incurred by not using

the appropriate difference between z_{0h} and z_{0m} may not be significant. Since experimentally z_{0h} is not well known, we have chosen to set $z_{0h} = z_{0m} = z_0$.

The functions GH and FH under unstable conditions are defined as (Louis 1979; Louis et al. 1982)

$$\mathrm{FH} = 1 - 10\,\mathrm{Ri}_B\left[1 + 7.5\frac{k^2}{\ln(z/z_{0m})\ln(z/z_{0m})} \times 10\left(-\mathrm{Ri}_B\frac{z}{z_{0m}}\right)^{0.5}\right]^{-1}, \quad (15)$$

$$\mathrm{GH} = 1 - 15\,\mathrm{Ri}_B\left[1 + 7.5\frac{k^2}{\ln(z/z_{0m})\ln(z/z_{0h})} \times 10\left(-\mathrm{Ri}_B\frac{z}{z_{0m}}\right)^{0.5}\right]^{-1}, \quad (16)$$

where Ri_B is the bulk Richardson number for surface layer, which is given by

$$\mathrm{Ri}_B = \frac{gz[\theta_v(z) - \theta_v(z_0)]}{\theta_v(z)u^2}, \quad (17)$$

where θ_v is the virtual potential temperature.

A number of investigations have been carried out to develop a relationship between the soil heat flux density and net radiation. Fuchs and Hadas (1972) suggested that for bare soil it can be described as

$$G = C_g R_n, \quad (18)$$

where the constant C_g is found to vary from 0.1 to 0.5 (Idso et al. 1975; Novak and Black 1983; Clothier et al. 1986), depending on the soil moisture and vegetation cover. Clothier et al. (1986) found that over alfalfa areas soil moisture does not have a significant effect on C_g. They also found that the soil heat flux density was related to the vegetation index.

From observations, Daughtry et al. (1990) showed that soil heat flux density could be related to NDVI and net radiation. They suggested that the relationship initially proposed by Kustas and Daughtry (1990) had the lowest error wherein

$$G = (0.325 - 0.208\mathrm{NDVI})R_n \quad (19)$$

and NDVI is expressed as

$$\mathrm{NDVI} = \frac{R_2 - R_1}{R_2 + R_1}, \quad (20)$$

where R_1, R_2 are the reflectances of channels 1 and 2, respectively, using preflight calibration and no atmospheric correction.

3. Experimental results

The model was evaluated against independent datasets from two relatively homogeneous sites at Hincks Park on the Eyre Peninsula of South Australia (Fig. 1) and the Lake King district of Western Australia (Fig. 2). Both sites lie in semiarid regions and are characterized by woodland areas composed of eucalyptus tree species with a mallee growth habit caused by several stems growing from an underground root stock and with an understory of sclerophyllous shrubs about 1 m high, principally of the genera *Acacia, Melaleuca,* and *Grevillea.* The adjoining farmlands are devoted to raising crops of winter wheat and limited grazing. Hincks Park is a 700–1000-km^2 conservation area in the midst of agricultural land, whereas Lake King represents the eastern extremity of agricultural development in Western Australia and is bounded by a vermin-

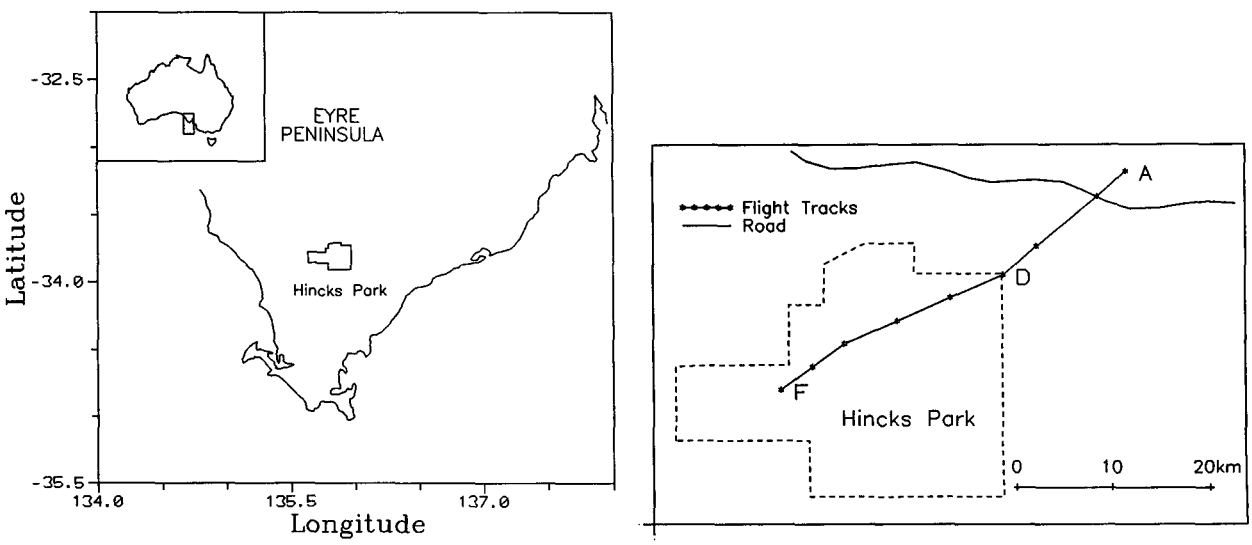

FIG. 1. Location of Hincks Park and the experimental flight track. Ground stations were located at AF.

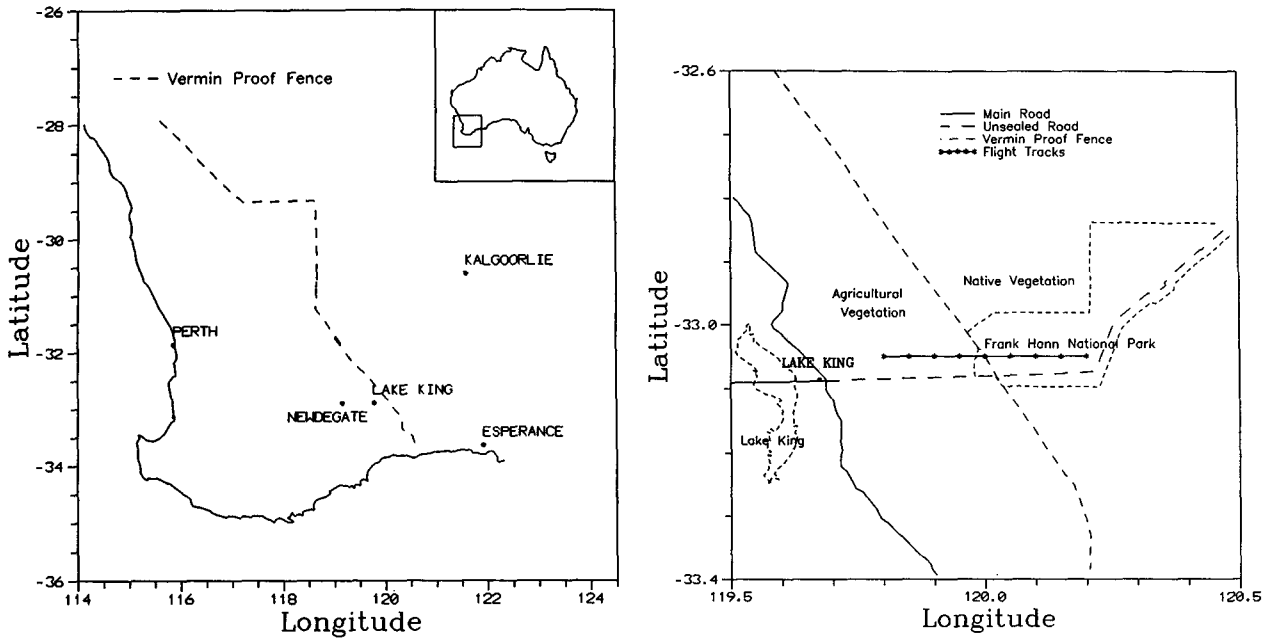

FIG. 2. Location of Lake King and experimental flight track.

proof fence that forms a natural demarcation between agricultural and native vegetation.

Four clear days (Hincks Park: 6 March 1988 and 4 December 1989 between harvesting and planting; Lake King: 30 August 1991 and 31 August 1991 during the crop-growing season) were chosen to evaluate the model. Figure 3 illustrates the NDVI at both sites for these periods and highlights the boundary between agricultural and native vegetation as well as the seasonal fluctuation in fractional green vegetation cover observed over the agricultural region in contrast to the marked constancy of the native vegetation.

At Lake King, sensible and latent heat flux density was calculated from fluxes evaluated by a GROB G109A single-engine motorglider (Hacker and Schwerdtfeger 1988; Hacker 1988). The aircraft measured infrared surface temperature, humidity, potential temperature, and the wind components at 13 Hz on horizontal traverses at heights of approximately 13 and 170 m. All flux data were subjected to a high-pass Lanczos filter to remove the mean, and the fluxes were averaged over 20 km. Albedo and NDVI were calculated from *NOAA-11* AVHRR data from the afternoon satellite overpass. The individual satellite pixels, with a resolution of 1 km, were also averaged over 20 km for both the native and agricultural vegetation.

At Hincks Park on 4 December, sensible and latent heat fluxes were measured by Bowen ratio and other

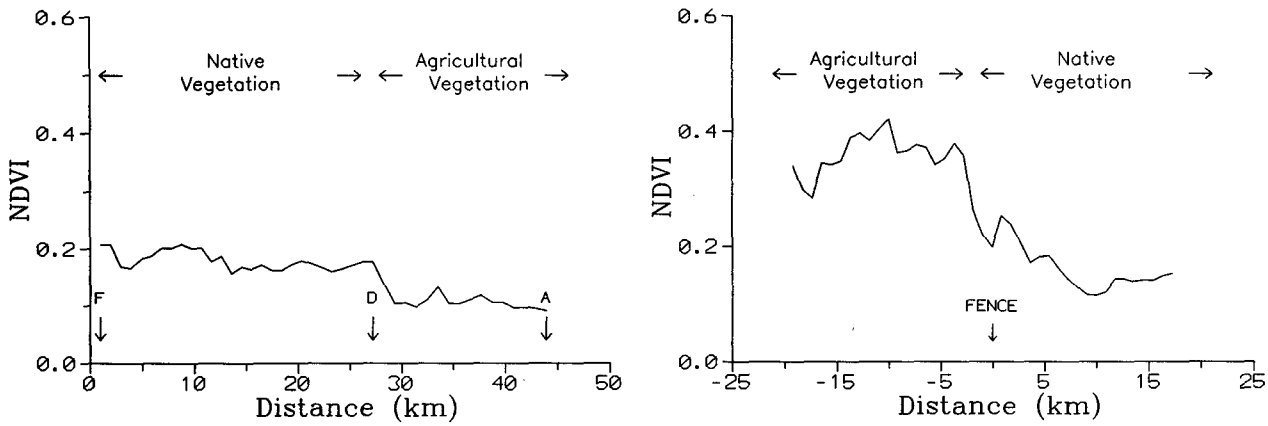

FIG. 3. Observed NDVI along flight track from *NOAA-11* at (a) Hincks Park on 4 December 1989 (*A*, *D*, and *F* correspond to positions along the flight track as shown in Fig. 1) and (b) Lake King on 31 August 1992.

meteorological data were collected at 1 m above the surface at the ground stations shown as *AF* in Fig. 1. Albedo, surface temperature, and NDVI were estimated from the *NOAA-11* AVHRR afternoon overpass. On 3 March, the sensible and latent heat fluxes were measured by the GROB aircraft and surface meteorological data were observed at 11 m (Williams 1991). Surface temperature was estimated from the *NOAA-9* afternoon overpass. The albedos and NDVI measured on 4 December were assumed for this day as the land surface conditions were similar with only dried-out stubble in the agricultural area and Fig. 3 illustrates the lack of any marked seasonal change in these values for the native vegetation.

Aircraft observations were used at both sites to estimate the friction velocity u_* and Monin–Obuhov length L by noting

$$u_* = (\overline{u'w'}^2 + \overline{v'w'}^2)^{0.25}, \quad (21)$$

where u', v', w' are the velocity component fluctuations about the mean, and

$$L = \frac{\theta_v u_*^3}{gk(\overline{w'\theta_v'})}. \quad (22)$$

These were used to evaluate the surface roughness given that

$$u = \frac{u_*}{k}\left[\ln\left(\frac{z}{z_{0m}}\right) + \psi_m\left(\frac{z}{L}\right)\right], \quad (23)$$

and for the unstable ($z/L < 0$) conditions pertaining at the time of the afternoon satellite overpass

$$\psi_m\left(\frac{z}{L}\right) = -2\ln\left[\frac{(1+x)}{2}\right] - \ln\left[\frac{(1+x^2)}{2}\right] + 2\tan^{-1}(x) - \frac{\pi}{2} \quad (24)$$

with (Businger 1973)

$$x = \left[1 - 15\left(\frac{z}{L}\right)\right]^{1/4}. \quad (25)$$

All model input data are summarized in Table 1.

The observed and model-predicted values of H, LE, and H + LE are shown in Figs. 4, 5, and 6. Sensible heat flux densities show good agreement with the aircraft observations ranging from surfaces where the sensible heat flux dominated to those where the latent flux dominated. Previous studies have noted systematic losses in the aircraft measurements of energy fluxes when compared to point measurements (i.e., Schuepp et al. 1987) suggesting that some flux transfer may be at length scales much longer than those associated with the atmospheric boundary layer (Shuttleworth 1991). However, this study essentially compares fluxes eval-

TABLE 1. Model input data.

	Hincks Park			Lake King	
	6 March 1988		4 December 1989	31 August 1991	
	Agricultural	Native	Native	Agricultural	Native
NDVI	0.07	0.15	0.15	0.36	0.15
Albedo	0.19	0.12	0.12	0.17	0.08
z_0 (m)	0.0028	0.044	0.044	0.0046	0.15

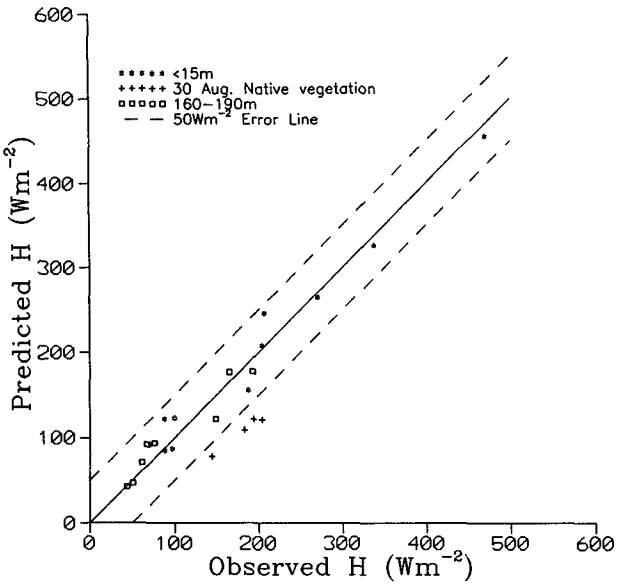

FIG. 4. Comparison between modeled and observed sensible heat flux density H.

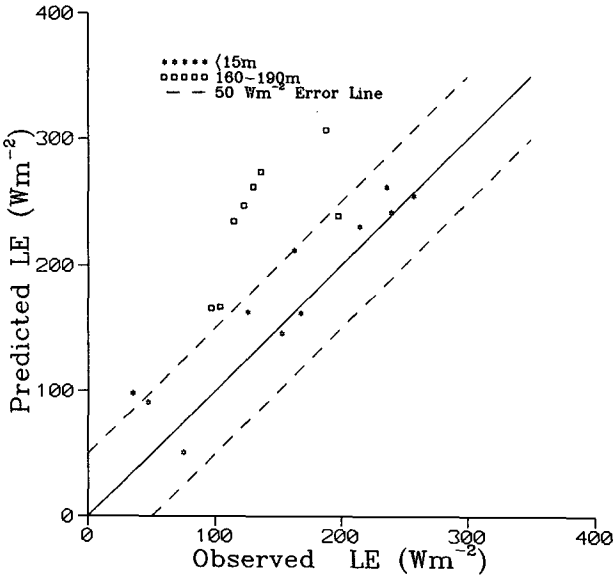

FIG. 5. Comparison between modeled and observed latent heat flux density LE.

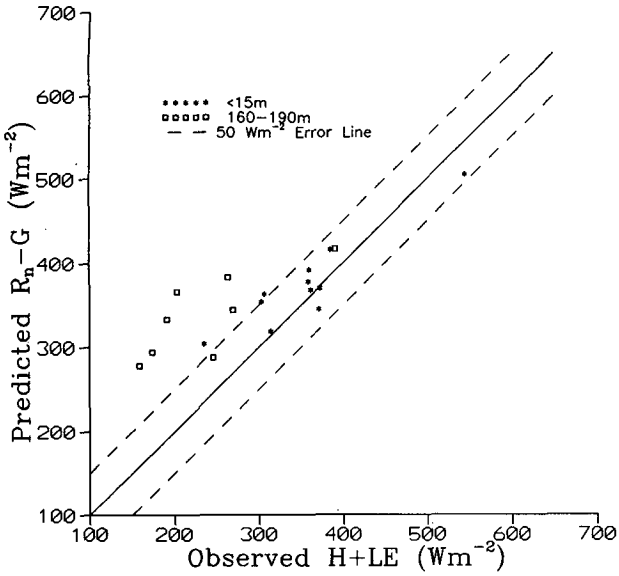

FIG. 6. Comparison between modeled ($R_n - G$) and observed ($H + LE$).

uated over similar spatial scales and the agreement between approaches is heartening.

The predicted sensible heat flux for the native vegetation on 30 August is lower than expected. However, the specific humidity observations (Fig. 7) suggest that moisture was advected from the agricultural area over the native vegetation under a westerly wind of 5.4 m s^{-1} during the afternoon; hence, the predicted fluxes are not representative of the native vegetation. Our model has also specifically neglected the effects of advection. The latent flux estimates are in agreement with observations made below 15 m and the sum of available energy $R_n - G$ shows reasonable agreement with the observations $H + LE$ below 15 m, but there is considerable divergence in the flux densities aloft. It should also be noted that we have neglected photosynthesis and energy storage within the vegetation layer as these fall within our experimental uncertainty.

Figure 8 illustrates the close agreement between the satellite-estimated radiant surface temperature and that measured by the aircraft at Lake King. The spikes in the aircraft observations result from local roads, etc., which are not resolvable by the satellite. Thus satellite-estimated surface temperatures are realistic for sensible heat flux calculations. The predicted flux densities using the NOAA AVHRR-derived radiant surface temperature are listed in Table 2. Errors shown for the sensible heat flux density result from variations in surface temperature, as measured by the satellite, across the 20-km pathlength, whereas the errors shown for the latent flux density are the result of scatter in both NDVI and albedo across the 20-km path as well as the scatter in the sensible heat flux density estimates. To some extent these errors highlight variations in average surface properties over the relatively homogeneous terrain. Nevertheless, the mean values show a realistic comparison to the spatially averaged aircraft fluxes for both the agricultural and native vegetation.

4. Discussion

The estimated available energy $R_n - G$ is in agreement with the observations $H + LE$ near the surface, while showing significant differences with the aircraft observations above 160 m (Fig. 6). Consequently, latent heat fluxes estimated from the satellite data are reasonable only near the ground and have larger errors aloft (Fig. 5). This indicates that in the absence of advection, the model produces useful results in the

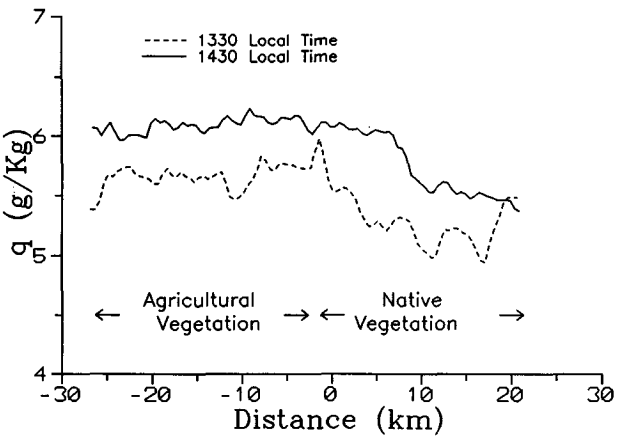

FIG. 7. Specific humidity measured by the aircraft along flight path on 30 August 1992 showing advection of moisture toward native vegetation.

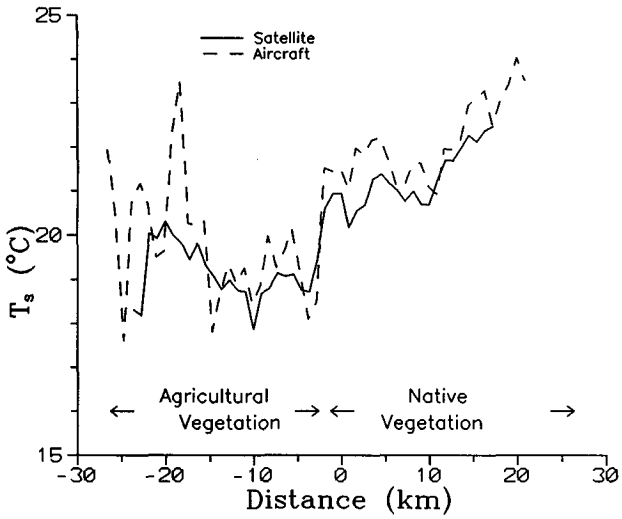

FIG. 8. Radiant surface temperature as measured by the aircraft between 1425 and 1448 LST and the satellite at 1504 LST 31 August 1991 at Lake King.

TABLE 2. Comparison of heat flux densities (W m^{-2}) measured at the surface and estimated from satellite surface temperature. All fluxes have been averaged over a homogeneous flight length of 20 km and the standard deviation of the satellite observations has been used to estimate the accuracy of the satellite-model determination.

Date	Site	Time (LST)		Heat flux density (W m^{-2})		
				H	LE	H + LE
4 December 1989	Hincks Park native	1400–1500	Bowen ratio observation	470	75	545
		1353	Model + satellite	455 ± 29	51 ± 42	505
6 March 1988	Hincks Park native	1405–1445	Aircraft observation	338	47	385
		1437	Model + satellite	326 ± 28	76 ± 38	402
	Hincks Park agricultural	1405–1445	Aircraft observation	271	35	306
		1437	Model + satellite	265 ± 19	91 ± 29	358
31 August 1991	Lake King native	1241–1448	Aircraft observation	200	149	349
		1504	Model + satellite	121 ± 19	136 ± 27	257
	Lake King agricultural	1241–1448	Aircraft observation	87	212	299
		1504	Model + satellite	71 ± 12	178 ± 20	249

surface layer but cannot account for the flux divergence above the surface layer.

Satellite measurements of NDVI and albedo were used to estimate the available energy. Thus, errors in the calibration of the satellite instruments and corrections for atmospheric transmission and land surface effects will influence these parameters. However, assuming a net radiation of 600 W m^{-2} and changing the NDVI by 0.1 leads to a change in $R_n - G$ of approximately 3%, showing that the model is not very sensitive to NDVI.

The sensitivity to albedo is more difficult to estimate because of the correction from narrow band to broad band as well as atmospheric transmission and the view angle. A 0.1 error in the overall estimated albedo would result in approximately a 15% error in available energy. The inaccuracy in albedo and net radiation contributes the bulk of the error in available energy. As soil heat flux is estimated to be less than $0.4R_n$, the errors in calculated available energy $R_n - G$ caused by errors in NDVI are small compared with the errors in the albedo.

Most radiant energy is transferred to sensible and latent heat flux; hence, accurate modeling of the sensible heat flux is important for latent heat estimation. Sensible heat is controlled by the difference between the aerodynamic potential temperature and air potential temperature as well as the surface exchange coefficient for heat. Therefore, any errors in calculating the sensible heat depend on the aerodynamic temperature, heat exchange coefficient, and surface temperature. Consequently, three methods for estimating the sensible heat flux were compared with the observations.

In addition to calculating the sensible heat flux density, H_1, from the aerodynamic potential temperature as defined by 8 and assuming $z_{0m} = z_{0h}$, the sensible heat flux density was also estimated using the surface potential temperature as

$$H_2 = \rho C_p C_h(z_{0m}, z_{0h}, \mathrm{Ri}_B)(\theta_s - \theta_a)$$
$$z_{0m} = 10 z_{0h} \tag{26}$$

and

$$H_3 = \rho C_p C_h(z_0, \mathrm{Ri}_B)(\theta_s - \theta_a)$$
$$z_{0m} = z_{0h} = z_0, \tag{27}$$

where for H_2 and H_3, the bulk Richardson number has been evaluated as

$$\mathrm{Ri}_B = \frac{gz[\theta_v(z) - \theta_{sv}]}{\theta_v(z)u^2}, \tag{28}$$

where θ_{sv} is the surface virtual potential temperature.

The resulting estimates of sensible heat flux density are given in Table 3 for Lake King and shown in Figs. 9 and 10 as a function of surface roughness and the difference between the radiative surface potential temperature and air potential temperature ($\theta_s - \theta_a$).

Table 3 shows that H_3 overestimates the sensible heat flux density and this becomes more marked as the surface roughness increases. Further, H_3 is considerably larger than H_1 or H_2 when z_{0m} is greater than 0.02 m (Fig. 9). Thus, the use of surface temperature and the assumed equivalence of z_{0m}, z_{0h} is only appropriate when both surface roughness and $\theta_s - \theta_a$ are small. Garratt and Hicks (1973) and Garratt (1978), among others, have shown that z_{0h} is less than z_{0m}, and Brutsaert (1982) suggested that z_{0h}/z_{0m} is of the order $1/12$–$1/2$ depending on the underlying surface. Recently, Beljaars and Holtslag (1991) observed z_{0h}/z_{0m} as 1/64 000 and Duynkerke (1992) showed that

TABLE 3. Comparison of sensible heat flux density calculated as H_1, H_2, and H_3 (W m^{-2}) with observations from three low-level flights between 1241 and 1448 LST 31 August 1991 at Lake King.

		Run 2	Run 3	Run 5
Agricultural				
z_{0m} = 0.0046 m	Observed	100	88	71
	H_1	123	122	92
	H_2	95	93	72
	H_3	137	136	102
	$T_s - T_a$ (°C)	5.6	5.9	4.3
Native				
z_{0m} = 0.15 m	Observed	207	204	188
	H_1	246	208	156
	H_2	368	298	219
	H_3	562	464	338
	$T_s - T_a$ (°C)	7.4	6.9	5.6

this ratio was also dependent on the leaf-area index and Prandtl number. Hence, the definition of surface temperature as $T(z_{0h})$ is problematic without sophisticated surface observations.

Figures 9 and 10 show that when z_{0m} is about 0.05 m, H_1 and H_2 give similar results; however, H_2 is very sensitive to z_{0m} and $\theta_s - \theta_a$ as z_{0m} increases above 0.05 m, while H_1 is not very sensitive to z_{0m}. For $z_{0m} > 0.05$ m, H_2 is more sensitive to $\theta_s - \theta_a$ than H_1. In other words, the use of H_2 requires a more accurate determination of the surface temperature to achieve the same accuracy in the sensible heat flux.

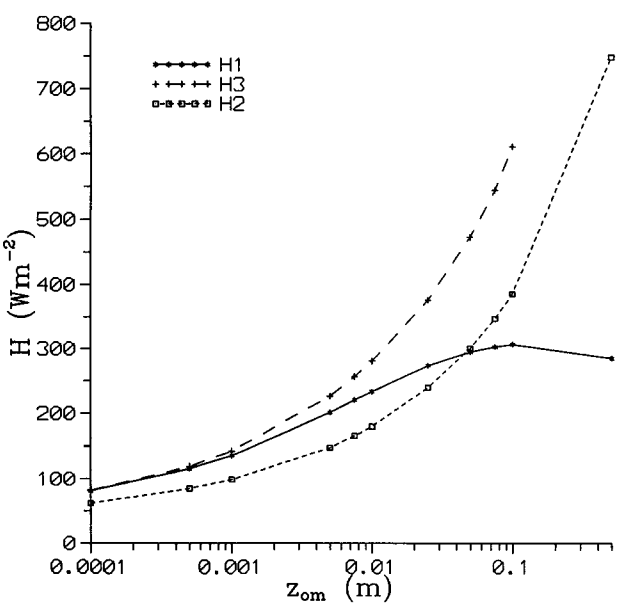

FIG. 9. Effect of variation of surface roughness on estimated sensible heat flux density (u = 5 m s^{-1}, $\theta_s - \theta_a$ = 10 K, z = 10 m).

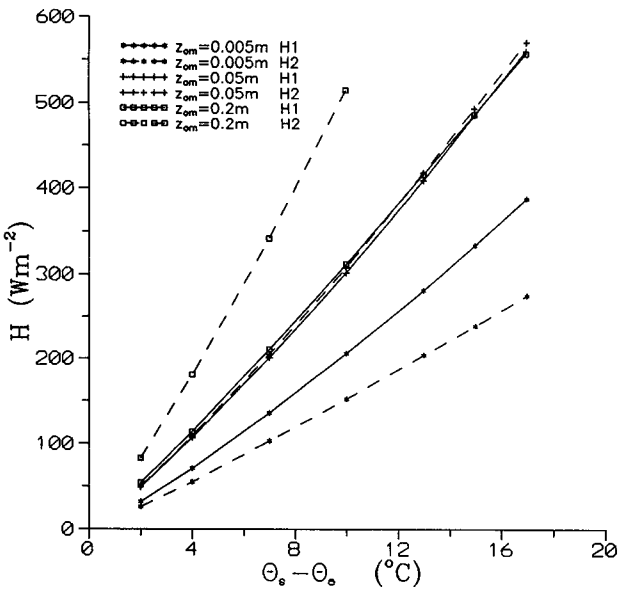

FIG. 10. Effect of variation of $\theta_s - \theta_a$ on estimated sensible heat flux density (u = 5 m s^{-1}, z = 10 m, z_{0m} = 0.005 m, 0.05 m, 0.2 m).

Table 3 illustrates that for small surface roughness, both H_1 and H_2 are in agreement with the observations (agricultural vegetation), although H_2 gives a slightly better estimate. However, when the surface roughness increases over the native vegetation, H_1 gives a reasonable estimate of the observed heat flux density while H_2 significantly overestimates the sensible heat flux density. In general, H_1 gives a reasonable estimate for the sensible heat flux density under all situations. As H_2 is sensitive to both $\theta_s - \theta_a$ and surface roughness, z_{0h}/z_{0m} seems to be not only a function of surface roughness but also depend on $\theta_s - \theta_a$ or atmospheric stability.

5. Conclusions

Direct use of the radiative surface temperature to evaluate the sensible heat flux density causes large errors when the surface roughness and $\theta_s - \theta_a$ are high. One can, however, use the aerodynamic potential temperature instead of the infrared surface potential temperature and greatly improve the estimated sensible heat flux density. When applied to relatively homogeneous agricultural and native vegetation, the model yields realistic estimates of the large-scale sensible and latent heat flux densities in the surface layer for cases where either the sensible or latent heat fluxes dominate and in the absence of advection. It cannot account for flux divergence above the surface layer and the validation has been limited to early afternoon unstable conditions, corresponding to the satellite overpass. As LE has been evaluated as the residual of the energy

balance equation, improvements in its estimation are dependent upon improved estimates of R_n and G.

Acknowledgments. This study was supported by the Australian Research Council. Throughout it Huang Xinmei was in receipt of an Australian Overseas Postgraduate Research Award and the associated postgraduate stipend through Murdoch University. NOAA AVHRR data was kindly supplied by the Western Australian Satellite and Technology Applications Consortium (WASTAC). All of this assistance is gratefully acknowledged.

REFERENCES

Beljaars, A. C. M., and A. A. M. Holtslag, 1991: Flux parameterization over land surfaces for atmospheric models. *J. Appl. Meteor.*, **30,** 327–341.

Brest, C. L., and S. Goward, 1987: Deriving surface albedo measurements from narrow band satellite data. *Remote Sens.*, **8,** 351–367.

Brutsaert, W., 1982: *Evaporation into the Atmosphere.* Reidel, 299 pp.

Businger, J. A., 1973: Turbulent transfer in the atmosphere surface layer. *Workshop on Micrometeorology,* Amer. Meteor. Soc., 67–100.

Chen, T. S., and G. Ohring, 1984: On the relationship between clear sky planetary and surface albedos. *J. Atmos. Sci.*, **41,** 156–158.

Choudhury, B. J., R. J. Reginato, and S. B. Idso, 1986: An analysis of infrared temperature observation over wheat and calculation of latent heat flux. *Agric. For. Meteorol.*, **37,** 215–225.

Clothier, B. E., K. L. Clawson, P. J. Pinter Jr., M. S. Moran, R. J. Reginato, and R. D. Jackson, 1986: Estimation of soil heat flux from net radiation during growth of alfalfa. *Agric. For. Meteorol.*, **37,** 319–329.

Daughtry, C. S. T., W. P. Kustas, M. S. Moran, P. J. Pinter Jr., R. D. Jackson, P. W. Brown, W. D. Nichols, and L. W. Gay, 1990: Spectral estimates of net radiation and soil heat flux. *Remote Sens. Environ.*, **32,** 111–124.

Duynkerke, P. G., 1992: The roughness length for heat and other vegetation parameters for a surface of short grass. *J. Appl. Meteor.*, **31,** 579–586.

Fuchs, M., and A. Hadas, 1972: The heat flux density in a nonhomogeneous bare loessial soil. *Bound.-Layer Meteor.*, **3,** 191–200.

Garratt, J. R., 1978: Transfer characteristics for a heterogeneous surface of larger aerodynamic roughness. *Quart. J. Roy. Meteor. Soc.*, **104,** 491–502.

——, and B. B. Hicks, 1973: Momentum, heat, and water vapour transfer to and from natural and artificial surface. *Quart. J. Roy. Meteor. Soc.*, **99,** 377–387.

Hacker, J. M., 1988: The spatial distribution of the vertical energy fluxes over a desert lake area. *Aust. Meteorol. Mag.*, **36,** 235–243.

——, and P. Schwerdtfeger, 1988: *The FIAMS Research Aircraft System Description.* FIAMS Tech. Report No. 8, Flinders University of South Australia, 60 pp. [Available from Flinders Institute for Atmospheric and Marine Sciences, Flinders University of South Australia, GPO Box 2100, Adelaide, S.A. 5000, Australia.]

Hall, F. G., P. J. Sellers, D. E. Strebel, E. T. Kanemasu, R. D. Kelly, B. L. Blad, B. J. Markham, J. R. Wang, and F. Huemmrich, 1991: Satellite remote sensing of surface energy and mass balance: Results from FIFE. *Remote Sens. Environ.*, **35,** 187–199.

Idso, S. B., J. K. Aase, and R. D. Jackson, 1975: Net radiation-soil heat flux relations as influenced by soil water content variations. *Bound.-Layer Meteor.*, **9,** 113–122.

Kustas, W. P., and C. S. T. Daughtry, 1990: Estimation of soil heat flux/net radiation ratio from spectral data. *Agric. For. Meteor.*, **49,** 205–223.

Louis, J. F., 1979: A parametric model of vertical eddy fluxes in the atmosphere. *Bound.-Layer Meteor.*, **17,** 187–202.

——, M. Tiedtke, and J. F. Geleyn, 1982: *A short history of the operational PBL-parameterization of ECMWF.* Workshop on planetary boundary-layer parameterization, ECMWF. [Available from European Centre for Medium-Range Weather Forecasts, Shinfield Park, Reading, Berks., United Kingdom.]

Novak, M. D., and T. A. Black, 1983: The surface heat flux density of a bare soil. *Atmos.-Ocean,* **21,** 431–443.

Price, J. C., 1984: Land surface measurements from the split window channels of the NOAA 7 Advanced Very High Resolution Radiometer. *J. Geophys. Res.*, **89,** 7231–7237.

Satterlund, D. R., 1979: An improved equation for estimating longwave radiation from the atmosphere. *Water Resour. Res.*, **15,** 1649–1650.

Savijarvi, H., 1990: Fast radiation parameterization schemes for mesoscale and shortrange forecast model. *J. Appl. Meteor.*, **29,** 437–447.

Schuepp, P. H., R. L. Desjardins, J. I. MacPherson, J. Boisvert, and L. B. Austin, 1987: Airborne determination of regional water use efficiency and evapotranspiration: Present capabilities and initial field tests. *Agric. For. Meteorol.*, **41,** 1–19.

Shuttleworth, W. J., 1991: Insight from large-scale observational studies of land/atmosphere interactions. *Surv. Geophys.*, **12,** 3–30.

Smith, R. C. G., H. D. Barrs, and W. S. Meyer, 1989: Evaporation from irrigated wheat estimated using radiative surface temperature: An operational approach. *Agric. For. Meteorol.*, **48,** 331–344.

Thom, A. S., and H. R. Oliver, 1977: On Penman's equation for estimating regional evaporation. *Quart. J. Roy. Meteor. Soc.*, **103,** 345–357.

Williams, A. G., 1991: *Internal Stucture and Interactions of Coherent Eddies.* Ph.D thesis, Flinders University of South Australia. [Available from Flinders Institute for Atmospheric and Marine Sciences, Flinders University of South Australia, GPO Box 2100, Adelaide, S.A. 5000, Australia.]

Zilitinkevich, S. S., 1970: *Dynamics of the Atmospheric Boundary Layer.* Leningrad Gidrometeor., 291 pp.